Innovative: International Multi-disciplinary Journal of Applied Technology
(ISSN 2995-486X) VOLUME 03 ISSUE 11, 2025

MORPHOLOGICAL CHARACTERIZATION BY SCANNING ELECTRON MICROSCOPY (SEM) OF COMPOSITE ADSORBENTS DERIVED FROM PLANT HUSK WASTE: A BASIS FOR DEVELOPING ECO-FRIENDLY MATERIALS FOR POLLUTANT ADSORPTION

Karimova Zarifa[1*], Nurmurodov Tulqin[2]
[1,2]Navoi State University of Mining and Technology, Navoi, Uzbekistan
*E-mail: zarifa_karimova_90@mail.ru

Abstract:

This study investigates the morphological features, obtained by scanning electron microscopy (SEM), of individual activated carbons prepared from agricultural and fruit-processing wastes apricot stone shells, walnut shells and grape seed shells and of their three-component composite adsorbent. The samples were pyrolysed at 600 °C in an inert atmosphere, chemically activated with KOH, and converted into a composite by mechanical mixing in an equal mass ratio (1:1:1) followed by a secondary heat treatment (300 °C). SEM analysis revealed that each precursor forms a distinct carbon skeleton: the apricot pyrolysate showed an open cellular (honeycomb-like) structure (cell density 400–600 cells/mm²), the walnut pyrolysate a dense sponge-like 3D-interconnected structure (800–1000 cells/mm²), and the grape pyrolysate a lamellar (plate-like) and "Swiss-cheese" morphology. KOH activation opened the cell walls in all samples and generated submicron pores (200–500 nm). The composite developed a hybrid "cheese–cellular–plate" morphology, absent in any individual component, together with a zone rich in uniformly sized (1–2 μm) circular pores, which morphologically confirms the synergistic effect of compositing. The resulting granular commercial form (0.3–0.8 mm) indicates the potential of the composite for industrial-scale application.

Key words: Scanning Electron Microscopy (SEM), Composite Adsorbent, Activated Carbon, Apricot Stone Shell, Walnut Shell, Grape Seed Shell, Pyrolysis, KOH Activation, Hierarchical Porosity, Morphology, Wastewater Treatment

Introduction

The contamination of water resources by heavy metals, nutrient ions and organic pollutants remains one of the most serious environmental problems worldwide. Adsorption is among the most widely used and effective wastewater-treatment methods, and activated carbons with high specific surface area serve as the principal adsorbent. However, the high cost of commercial imported activated carbons (e.g., Norit, Calgon) limits their large-scale use in developing countries. For this reason, the

development of inexpensive and environmentally safe adsorbents from agricultural and fruit-processing wastes has become an important applied research direction in recent years [1][2][3][4][5].

In the Republic of Uzbekistan, large amounts of apricot stone, walnut and grape seed shells are generated annually as waste by the fruit-growing and processing industries. The high content of cellulose, hemicellulose, lignin, and polyphenolic and tannin compounds in these wastes makes them promising natural precursors for adsorbent materials. Converting such wastes into high-grade activated carbon and composite adsorbents is consistent with circular-economy principles and simultaneously addresses waste utilisation, import substitution, and protection of the hydrosphere[6][7][8].

The adsorption performance of activated carbons is directly related to their surface morphology, pore structure and surface area. Scanning electron microscopy (SEM) is one of the principal techniques for the visual and semi-quantitative assessment of these features, enabling direct observation of the macro-, meso- and microporous structure, the architecture of the cell walls, and the distribution of mineral residues. SEM is especially valuable for revealing the morphological changes and synergistic effects that arise when components from different sources are combined[9][10].

The aim of this study is to comparatively analyse, by SEM, the morphological features of activated carbons obtained from apricot stone, walnut and grape seed shells and of their three-component composite adsorbent, and to identify the morphological synergistic advantage of compositing. Each stage raw material, pyrolysis, KOH activation and composite formation was followed consistently from a morphological standpoint.

Materials and methods

Apricot stone shells, walnut shells and grape seed shells were used as raw materials. Each precursor was first washed, dried and ground. In the carbonisation step, the samples were pyrolysed at 600 °C in an inert atmosphere (N_2/Ar flow). The pyrolysis temperature (600 °C) was selected on the basis of differential thermal analysis (DTA/TG): this temperature is sufficient to form the mesoporous matrix of the apricot component while preserving the lignin-based aromatic skeleton of the walnut component. In the chemical-activation step, the pyrolysates were treated with potassium hydroxide (KOH) at 600–800 °C. KOH activation is an effective method for substantially increasing the specific surface area of biomass-based activated carbons and for creating ultramicropores [11][12][13]. During this process, KOH reacts with carbon according to the following main reactions:

$6KOH + 2C \rightarrow 2K + 3H_2 + 2K_2CO_3$

$K_2CO_3 \rightarrow K_2O + CO_2$; $K + CO_2 \rightarrow K_2O + CO$

The evolved H_2, CO and CO_2 gases escape under pressure from within the carbon layers, creating new micro- and ultramicropores; potassium metal intercalates between the layers and, after subsequent washing-out, leaves a high specific surface area exposed. After activation, the samples were washed until a neutral reaction was reached and then dried.

The composite adsorbent was prepared by mechanically mixing the three KOH-activated samples (apricot + walnut + grape) in an equal mass ratio (1:1:1) followed by a secondary heat treatment (300 °C, inert atmosphere, 2 h).

The surface morphology of the samples was studied by SEM at various magnifications (250×–35000×). The horizontal field width (HFW) was recorded for several images (e.g., HFW 414 µm at 500× and 104 µm at 2000× for the apricot pyrolysate). Cell density and pore sizes were estimated semi-quantitatively from the images. Raman spectroscopy parameters (D and G bands, I_D/I_G ratio, crystallite size La) are reported as data complementary to the SEM results; the graphite crystallite size was calculated using the Tuinstra–Koenig relation [14][15][16].

Results and Discussion

The SEM images of the raw grape seed shell (from the literature) showed a partly smoothed surface with numerous irregular macropores. A large crater-shaped depression (10–12 μm in diameter) was observed in the centre, surrounded by many fine pores (0.5–2 μm), indicating the bimodal porous nature of the material. At low magnification (250×), macropores 5–20 μm in size were seen on the surface of a single particle, containing finer meso- and micropores within them, forming a three-level hierarchical pore structure. This natural porosity provides a favourable basis for further development after pyrolysis and activation.

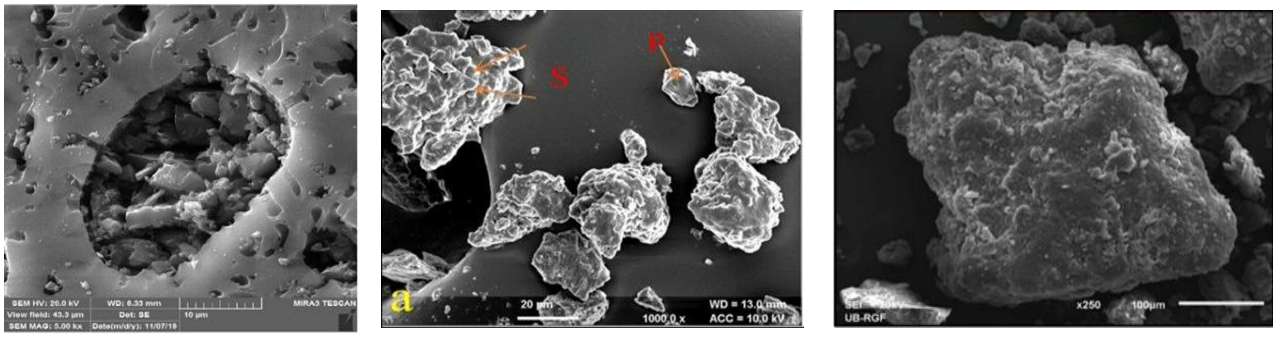

Figure 1. SEM images of grape seed husks at various magnification levels

Apricot stone shell pyrolysate. At 500× (HFW 414 μm), the sample surface had a uniformly distributed cellular (honeycomb-like) structure composed of polygonal open cells 20–50 μm in size, densely connected by walls. The morphology indicates that the natural conducting vessels (xylem) of the plant tissue were preserved after carbonisation. The cell density (400–600 cells/mm²) is a high macroporosity value for biomass-based activated carbons. At 2000× (HFW 104 μm), the cell walls displayed a delaminated lamellar morphology (wall thickness 0.5–2 μm, length 10–30 μm). Thin microcracks 5–15 μm long between the walls act as additional transport channels for the sorbate.

Walnut shell pyrolysate. At 500×, the sample surface had a dense, multilayered sponge-like open-cell structure. In contrast to the apricot sample, the cells were smaller and more densely packed (10–25 μm in diameter; density 800–1000 cells/mm²). At 2000×, the 3D architecture of the cell walls curved lamellae connected by arching bridges was observed. At 35000×, the bottom of a single cell (1.8 × 1.3 μm) was exposed, its inner surface showing a granular (lava-like) morphology densely covered with nodular structures 50–200 nm in size. These nano-scale nodules indicate that the lignin–juglone fraction formed aromatic clusters during pyrolysis. The dense, robust structure of the walnut pyrolysate is consistent with the high thermal stability indicated by the DTA data.

Grape seed shell pyrolysate. At 1200×, the sample surface had a compressed lamellar/leafy morphology, with carbon layers stacked horizontally. In sharp contrast to the apricot and walnut samples, no open cells or networks were present; cracks 3–10 μm deep between the layers act as horizontal channels. At 2500×, thousands of fine spherical and oval pores (0.3–1.5 μm in diameter) densely covered the surface, forming a “Swiss-cheese” morphology. Rod-like crystallites 2–5 μm long and 200–400 nm thick were also observed; these are residues of calcium oxalate (CaC_2O_4) or mineral salts, in which grape is naturally rich. At 10000×, a unique morphology combining three types of structure plate-like carbon sheets, hexagonal crystal rods (3–6 μm long), and open pores 2–4 μm deep was identified.

Apricot–KOH. At 500×, the sample surface had an open-cell, zeolite-like structure; in contrast to the pyrolysed-only sample, the cell interiors were considerably deeper and fully opened (15–40 μm). At 2000×, thousands of submicron pores (200–500 nm in diameter) were distributed across the cell-wall

surface like a honeycomb, indicating a sharp increase in specific surface area. At 15000×, two-level porosity was clearly visible: (1) oval mesopores 0.3–0.8 µm in diameter; and (2) spherical nanoparticles 50–150 nm in size on the surface (residual K-compounds or graphitic nanoblocks).

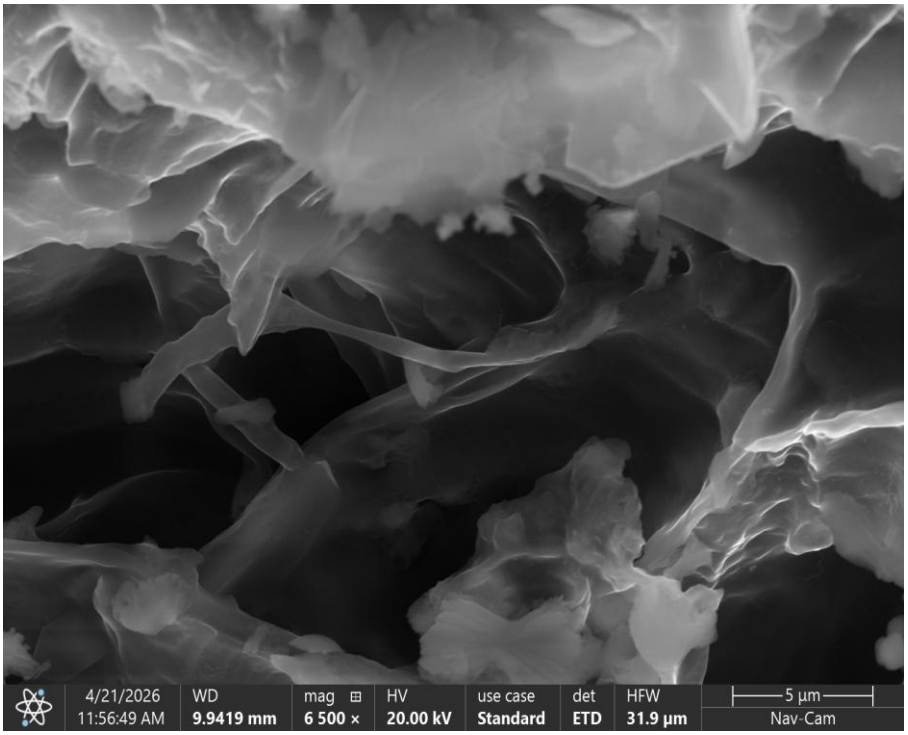

Figure 2. KOH-activated grape seed husk SEM (6500×)

Walnut–KOH. At 500×, the distinct open cells of the pyrolysed-only walnut sample had disappeared entirely, replaced by a disordered, folded morphology resembling a cerebriform or mountain-ridge pattern; long, thin bright lines (graphitic ridges) on the surface formed a network structure. At 2500×, a 3D-interconnected carbon skeleton was observed: carbon lines 1–2 µm thick formed "Y-" and "X-shaped" junctions, leaving macropores 3–8 µm in size between them. At 35000×, exfoliated graphitic sheets (thickness < 100 nm) and deep crack-channels between them (1–2 µm deep, 100–300 nm wide) were identified.

Grape–KOH. At 1500×, the plate-like and Swiss-cheese morphology of the pyrolysed-only grape sample had been completely reshaped into a cobblestone-pavement-like structure; rounded mounds 3–8 µm in size were densely distributed over the surface. The CaC_2O_4 crystal rods from pyrolysis were recrystallised by KOH into spherical particles 1–4 µm in size. At 6500×, the most distinctive feature of the grape–KOH sample a delaminated, graphene-like layered structure was observed: layers < 100 nm thick and 5–10 µm long were stacked on one another, forming large open interlayer voids 2–4 µm deep.

In the SEM images of the composite adsorbent, a hybrid "cheese–cellular–plate" morphology, absent in any of the individual components, was identified. A thick, broad plate-like fragment (10–15 µm) a stacked graphene-like layer originating from the grape–KOH component was observed in the centre of the image; above it, thousands of ordered, uniformly sized (1–2 µm) circular pores were very densely arranged, exhibiting a honeycomb morphology. This zone rich in uniformly sized pores is a new, reinforced porous region that arises specifically from compositing and is not found in any individual component sample.

The composite, in powder form, was shown as three independent fragments 20–60 µm in size. In the image, the "P" (macropore, 5–15 µm) and "S" (rough, cauliflower-like fragment surface) markings

indicate two levels of the composite structure. The similar morphology of the three fragments shows that the composite was prepared homogeneously and that all three components were evenly distributed. Macroscopically, the composite consists of uniformly sized light-brown granules 0.3–0.8 mm in size, indicating its technological readiness for industrial-scale application (direct use in filter columns).

The composite differed from the individual components in all the main Raman parameters: I_D/I_G = 1.07 (highest), La = 4.11 nm (smallest), Valley/G = 0.56 (lowest), and a background level of 14,350 counts (about twice as clean). These indicators are fully consistent with the hybrid morphology and reinforced porous zone observed by SEM.

The SEM results showed that each precursor makes a distinct morphological contribution to the formation of the carbon skeleton. With its open cellular (honeycomb) structure, the apricot pyrolysate provides a mesoporous matrix and fast transport channels for the sorbate; the walnut pyrolysate, with its dense, aromatic-rich 3D-interconnected skeleton, provides mechanical strength and microporosity; and the grape pyrolysate, with its plate-like and "Swiss-cheese" morphology and mineral residues (CaC_2O_4), serves as selective adsorption sites. These features complement one another.

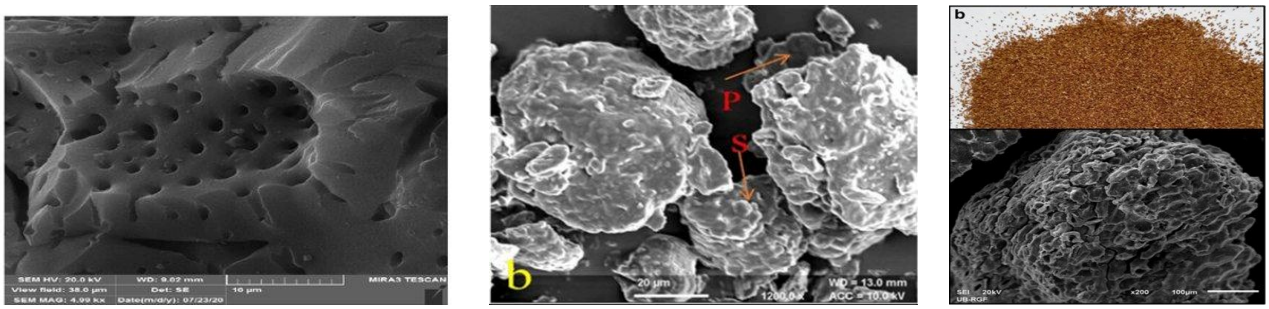

Figure 3. SEM image of a three-component composite adsorbent

KOH activation caused significant morphological changes in all samples: the cell walls opened, submicropores and mesopores formed, and in the walnut sample the cells "melted" and were reshaped into a 3D-interconnected skeleton. These results are consistent with the pore-forming mechanism of KOH activation: new pores open and the surface area increases through intercalation and gas evolution [3]. The wide distribution of submicron pores observed by SEM is consistent with the increase in the I_D/I_G ratio in the Raman data (an increase in the density of active sites).

The hybrid "cheese–cellular–plate" morphology and the new zone rich in uniformly sized circular pores identified in the composite morphologically confirm the synergistic effect of compositing. The combination of the three components is expected to form a four-level porosity system: macropores (mainly from grape), mesopores (mainly from apricot), micropores (mainly from walnut), and ultramicropores resulting from KOH activation. Such a hierarchical structure may simultaneously provide fast sorbate transport, wide diffusion channels and high uptake capacity.

The morphological diversity is also significant from an adsorption standpoint. The surface structure of each component is associated with a different mechanism: the microporous skeleton of the walnut component is expected to provide physical adsorption, the oxygen-containing functional groups of the apricot component chemisorption, and the polyphenol residues of the grape component selective uptake of heavy-metal ions through chelate binding. The four-level porosity system identified by SEM allows these mechanisms to be combined in a single material, providing a morphological basis for the broad-spectrum uptake of heavy metals (Pb^{2+}, Cd^{2+}, Cu^{2+}, Cr^{6+}, etc.), nutrient ions (NH_4^+, NO_3^-, PO_4^{3-}) and organic pollutants [4, 5].

The recrystallised mineral particles ($CaC_2O_4/CaCO_3$ residues) and the graphene-like delaminated layers observed in the grape–KOH sample may confer additional selectivity and stability over a wide

pH range on the composite. In addition, the granular commercial form of the composite (0.3–0.8 mm) offers practical advantages in that it does not generate dust and can be used directly in filter columns. Such a locally sourced adsorbent enables the substitution of imported activated carbons and the implementation of circular-economy principles.

It should be emphasised that, although the high specific surface area reported in the literature for biomass-based KOH-activated carbons (typically up to 2000–3000 m^2/g [3]) is morphologically plausible, the specific surface area, total pore volume and adsorption capacity of the present composite are projected (expected) values based on the morphological observations and were not measured directly by BET or adsorption experiments within this work. Numerical confirmation requires N_2 adsorption–desorption isotherms (BET, BJH, DFT) and adsorption experiments with model pollutants (Pb^{2+}, Cd^{2+}, dyes, etc.). This is the task of the next stage of the research.

Conclusions

SEM analysis consistently revealed the morphological features of the activated carbons based on apricot stone, walnut and grape seed shells and of their composite, supporting the following main conclusions:

1. In their natural state the raw materials have distinct morphologies: the grape seed shell exhibits bimodal and hierarchical porosity. This natural porosity provides a basis for development after pyrolysis and activation.
2. After pyrolysis at 600 °C, all three samples transformed from amorphous biomass into an ordered carbon matrix: apricot open cellular (honeycomb, 400–600 cells/mm^2); walnut dense sponge-like 3D network (800–1000 cells/mm^2); grape plate-like and "Swiss-cheese" morphology.
3. KOH activation opened the cell walls in all samples, generated submicron (200–500 nm) and mesopores, and substantially increased the surface area; a 3D-interconnected structure formed in walnut–KOH and a graphene-like delaminated layered structure in grape–KOH.
4. A hybrid "cheese–cellular–plate" morphology and a new zone rich in uniformly sized (1–2 µm) circular pores absent in any individual component were identified in the composite, morphologically confirming the synergistic effect of compositing.
5. The granular commercial form of the composite (0.3–0.8 mm) indicates its technological readiness for industrial-scale use (in filter columns).
6. On the basis of the morphological observations, the specific surface area and adsorption capacity of the composite are expected to be high; confirming these projections requires BET analysis and adsorption experiments at the next stage.

References

[1] J. Wang and S. Kaskel, "KOH activation of carbon-based materials for energy storage," *Journal of Materials Chemistry*, vol. 22, no. 45, pp. 23710–23725, 2012, doi: 10.1039/C2JM34066F.

[2] M. Sevilla, N. Díez, and A. B. Fuertes, "More sustainable chemical activation strategies for the production of porous carbons," *ChemSusChem*, vol. 14, no. 1, pp. 94–117, 2021.

[3] M. Sevilla and R. Mokaya, "Energy storage applications of activated carbons: Supercapacitors and hydrogen storage," *Energy & Environmental Science*, vol. 7, no. 4, pp. 1250–1280, 2014.

[4] M. Zhou *et al*., "Nitrogen-doped porous carbons through KOH activation with superior performance in supercapacitors," *Carbon*, vol. 68, pp. 185–194, 2014.

[5] Y. Lv *et al*., "A comprehensive study on KOH activation of ordered mesoporous carbons and their supercapacitor application," *Journal of Materials Chemistry*, vol. 22, no. 1, pp. 93–99, 2012.

[6] Y. Li *et al*., "Ultrahigh surface area hierarchical porous carbon derived from biomass via a new

KOH activation strategy for high-performance supercapacitor," *International Journal of Hydrogen Energy*, vol. 49, pp. 67–80, 2024.

[7] A. Bhatnagar and M. Sillanpää, "Utilization of agro-industrial and municipal waste materials as potential adsorbents for water treatment – A review," *Chemical Engineering Journal*, vol. 157, no. 2–3, pp. 277–296, 2010, doi: 10.1016/j.cej.2010.01.007.

[8] A. Bhatnagar, M. Sillanpää, and A. Witek-Krowiak, "Agricultural waste peels as versatile biomass for water purification – A review," *Chemical Engineering Journal*, vol. 270, pp. 244–271, 2015.

[9] A. A. Aryee *et al*., "A review on functionalized adsorbents based on peanut husk for the sequestration of pollutants in wastewater: Modification methods and adsorption study," *Journal of Cleaner Production*, vol. 310, Art. no. 127502, 2021.

[10] N. H. Solangi *et al*., "Development of fruit waste derived bio-adsorbents for wastewater treatment: A review," *Journal of Hazardous Materials*, vol. 416, Art. no. 125848, 2021.

[11] A. K. Tolkou *et al*., "Comparison of modified peels: Natural peels or peels-based activated carbons for the removal of several pollutants found in wastewaters," *C*, vol. 10, no. 1, Art. no. 22, 2024.

[12] F. Tuinstra and J. L. Koenig, "Raman spectrum of graphite," *Journal of Chemical Physics*, vol. 53, no. 3, pp. 1126–1130, 1970, doi: 10.1063/1.1674108.

[13] A. C. Ferrari and J. Robertson, "Interpretation of Raman spectra of disordered and amorphous carbon," *Physical Review B*, vol. 61, no. 20, pp. 14095–14107, 2000, doi: 10.1103/PhysRevB.61.14095.

[14] A. C. Ferrari and J. Robertson, "Resonant Raman spectroscopy of disordered, amorphous, and diamond-like carbon," *Physical Review B*, vol. 64, no. 7, Art. no. 075414, 2001.

[15] M. Ramsteiner and J. Wagner, "Resonant Raman scattering of hydrogenated amorphous carbon: Evidence for π-bonded carbon clusters," *Applied Physics Letters*, vol. 51, no. 17, pp. 1355–1357, 1987.

[16] M. Yoshikawa *et al*., "Resonant Raman scattering of diamond-like amorphous carbon films," *Applied Physics Letters*, vol. 52, no. 19, pp. 1639–1641, 1988.